



RESEARCH LETTER

10.1002/2014GL062791

Key Points:

- New method allows 3-D analysis of magnetic data collected by deep-sea submersible
- It provides absolute magnetization intensity and polarity of shallow subseafloor
- Nonmagnetic sulfides shape deep-sea magnetics at basalt-hosted hydrothermal site

Correspondence to:

J. Dyment,
jdy@ippg.fr

Citation:

Szitkar, F., J. Dyment, Y. Fouquet, Y. Choi, and C. Honsho (2015), Absolute magnetization of the seafloor at a basalt-hosted hydrothermal site: Insights from a deep-sea submersible survey, *Geophys. Res. Lett.*, *42*, doi:10.1002/2014GL062791.

Received 8 DEC 2014

Accepted 21 JAN 2015

Accepted article online 23 JAN 2015

Absolute magnetization of the seafloor at a basalt-hosted hydrothermal site: Insights from a deep-sea submersible survey

Florent Szitkar¹, Jérôme Dyment¹, Yves Fouquet², Yujin Choi¹, and Chie Honsho³

¹Institut de Physique du Globe de Paris, Sorbonne Paris Cité, Université Paris Diderot, CNRS UMR 7154, Paris, France,

²IFREMER Centre de Brest, Plouzané, France, ³Atmosphere and Ocean Research Institute, University of Tokyo, Kashiwa, Japan

Abstract The analysis of high-resolution vector magnetic data acquired by deep-sea submersibles (DSSs) requires the development of specific approaches adapted to their uneven tracks. We present a method that takes advantage of (1) the varying altitude of the DSS above the seafloor and (2) high-resolution multibeam bathymetric data acquired separately, at higher altitude, by an Autonomous Underwater Vehicle, to estimate the absolute magnetization intensity and the magnetic polarity of the shallow subseafloor along the DSS path. We apply this method to data collected by DSS *Nautile* on a small active basalt-hosted hydrothermal site. The site is associated with a lack of magnetization, in agreement with previous findings at the same kind of sites: the contrast between nonmagnetic sulfide deposits/stockwork zone and strongly magnetized basalt is sufficient to explain the magnetic signal observed at such a low altitude. Both normal and reversed polarities are observed in the lava flows surrounding the site, suggesting complex history of accumulating volcanic flows.

1. Introduction

The development of deep-sea submarine exploration involves different types of vehicles designed to perform specific tasks. Whereas larger-scale geophysical (including magnetic) and bathymetric surveys are generally acquired by autonomous underwater vehicles (AUVs) flying 50 to 100 m above the seafloor, near-seafloor dives aimed at direct geological observation and sample collection are achieved by either remotely operated vehicles (ROVs) or manned submersibles (hereafter collectively named deep-sea submersibles or DSSs). The DSSs, however, can also be equipped with magnetometers as their close proximity to the seafloor offers a unique opportunity to collect very high resolution magnetic data. The AUV magnetic data are generally acquired on long, regularly spaced parallel profiles at a constant altitude above seafloor, allowing the computation of magnetic anomaly grids. Conversely, DSS high-resolution vector magnetic data are measured along sinuous tracks at very variable altitudes (0–20 m above the seafloor), which make their analysis by the existing inversion methods not optimal [e.g., Parker and Huestis, 1974; Hussenöeder et al., 1995; Honsho et al., 2012]. However, Honsho et al. [2009] proposed a method suitable for such data acquired across elongated (2-D) magnetized bodies.

Here we improve this method and estimate the absolute magnetization of shallow subseafloor (up to ~ 20 m, depending on the altitude of the measurement) along the path of the DSS. The method takes full advantage of the varying altitude of the DSS but could also be used with any kind of deep-towed instrument able to carry a vector magnetometer and subject to altitude variations. In our case, the requested high-resolution bathymetric data are collected by the multibeam echosounder of an associated AUV, but top-end shipborne multibeam echosounder could be suitable for the task in a relatively shallow environment. We test this method on a data set collected over a small active basalt-hosted hydrothermal site discovered in 2012 in the Southwestern Pacific Ocean by DSS *Nautile* of Ifremer. Such low-altitude survey allows for much smaller features to be measured and detected compared to previous surveys [Tivey et al., 1993; Tivey and Johnson, 2002; Tivey and Dyment, 2010; Zhu et al., 2010; Caratori-Tontini et al., 2012; Nakamura et al., 2013; Honsho et al., 2013; Szitkar et al., 2014a, 2014b]. Because the data have been collected as part of an industrial project, the geographical coordinates of the site are confidential and will not be disclosed.

2. Data and Initial Processing

During an Ifremer scientific cruise in the Southwestern Pacific region in 2012, we collected high-resolution bathymetric and magnetic data using both AUV *Idef-X* and DSS *Nautile* of Ifremer. In a nested approach, the

AUV performed reconnaissance surveys and the DSS dove on specific targets. The AUV surveyed east-west parallel profiles 200 m apart, at an average altitude of 70 m above the seafloor. Bathymetric data were acquired using an EM2040 multibeam echosounder, whereas magnetic data were collected with a three-component fluxgate magnetometer mounted inside the nose of the AUV, away from the motor. The AUV line spacing was optimal for full bathymetric coverage but too wide apart for an appropriate mapping of the magnetic anomaly. Only wavelengths longer than 200 m could be correctly recovered, resulting in a rather poor resolution of the AUV magnetic maps. Despite this limitation, onboard processing of the AUV magnetic data allowed detecting a wide negative reduced-to-the-pole (RTP) anomaly possibly reflecting the characteristic lack of magnetization associated with the largest basalt-hosted hydrothermal areas [Tivey *et al.*, 1993; Tivey and Johnson, 2002; Sztikar *et al.*, 2014a]. Nevertheless, higher-resolution data, and therefore a survey closer to the seafloor, are desirable to detect smaller hydrothermal sites. With an average altitude of 0 to 20 m above the seafloor, DSS Nautilie is the perfect tool for such a detailed exploration.

The magnetic susceptibility tensors A (nine coefficients) and remanent magnetization vectors H_p (three coefficients) of the AUV and the DSS were estimated for each dive using the method developed by Isezaki [1986] and Honsho *et al.* [2009], based on “calibration loops” performed at the beginning of the dives, at distance from both the ship and the seafloor. Indeed, DSS Nautilie is naturally rotating during the descent and keeps the same average pitch during the whole dive, allowing these loops to be used for estimating its magnetic effect. Conversely, the AUV points downward during the descending loops, which are therefore not suitable to estimate its magnetic effect in the survey conditions. Specific, zero pitch loops are therefore carried out at the sea surface prior to the dive. We applied this approach to remove the magnetic effect of each vehicle from the raw data, converted the resulting vector magnetic field to geographical coordinates, and transformed it to vector magnetic anomaly by subtracting the main geomagnetic field approximated by the International Geomagnetic Reference Field model [International Association of Geomagnetism and Aeronomy Working Group V-MOD, 2010].

3. Inversion Method

Several methods have been proposed to invert magnetic anomalies into equivalent magnetization. Nevertheless, many of them are not suitable for near-seafloor, high-resolution surveys, as they require data collection on a datum plane [e.g., Parker and Huestis, 1974]. They are consequently used for surface measurements. Upward continuation of uneven deep-sea magnetic data to a datum plane above the highest point of the survey is achievable [Guspi, 1987] but results in a loss of the high-resolution data obtained in these kinds of surveys. Another approach considers an equivalent geometry with the acquisition on a datum plane and a virtual geometry of the seafloor [Pilkington and Urquhart, 1990; Hussenoeder *et al.*, 1995]. However, the computation remains approximate and does not allow sharp topographic or vehicle-track variations.

The most recent and promising inversion method for deep-sea magnetic data has been developed by Honsho *et al.* [2012]. Unlike other methods, this Bayesian approach is performed in the spatial domain, avoids any upward continuation (i.e., loss of resolution), and is adapted to uneven surveys following the shape of the seafloor. To date, this method has only been applied to a limited number of sites [Honsho *et al.*, 2013; Sztikar *et al.*, 2014a, 2014b], but these few examples confirm that resulting equivalent magnetization retains the high resolution of the magnetic anomalies.

A major drawback of these inversion methods is that they only allow for computing an equivalent magnetization by reference to a magnetized layer of constant thickness. As a consequence of the intrinsic nonuniqueness of the potential field problem, it is possible to calculate an annihilator, i.e., a magnetization distribution producing no magnetic anomaly for a given geometry of the experiment. Any appropriate distribution of equivalent magnetization can have any amount of annihilator added to it to produce another solution, and the final choice often depends on additional geological and geophysical considerations. The equivalent magnetization is therefore relative to both the chosen thickness of the magnetic layer and the amount of added annihilator. This quantity does not provide much information about the absolute magnetization of the seafloor, but merely about magnetization contrasts.

Honsho *et al.* [2009] adopted a different approach to analyze high-resolution vector magnetic data collected by DSS. Instead of trying to correct the magnetic anomaly for the complex geometry of the experiment, they took advantage of the uneven tracks of the vehicle and the rough seafloor topography to estimate the absolute magnetization of the seafloor. To do so, they compare the observed magnetic anomalies to synthetic anomalies

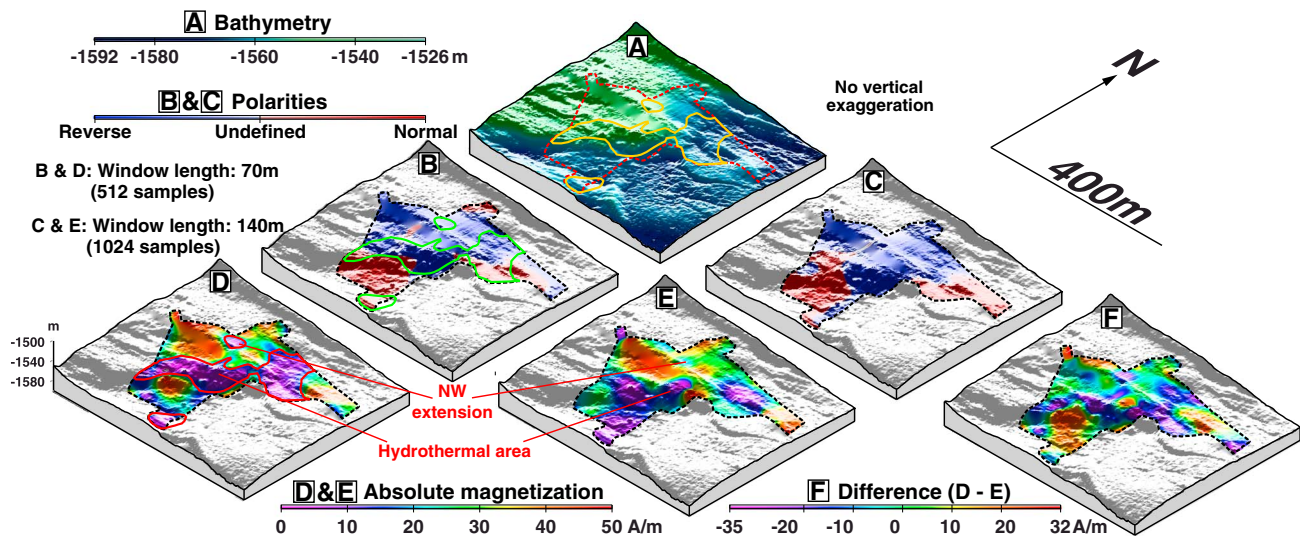


Figure 1. Bathymetry, magnetic polarity, and magnetization intensity over a small active basalt-hosted hydrothermal site: effects of the sliding window length. (a) High-resolution bathymetry, magnetic polarity assuming (b) a 70 m wide sliding window and (c) a 140 m wide sliding window, absolute magnetization computed for (d) a 70 m wide sliding window and (e) a 140 m wide sliding window, and (f) difference between Figures 1d and 1e underlining the loss of short wavelengths resulting from the use of wider sliding windows. Orange, green, and red lines on Figures 1a, 1b, and 1d, respectively delineate the hydrothermal area. On all panels, the dotted line encompasses the diving area. The northwestern extension of the site is clearly visible in Figure 1d but almost completely disappears in Figure 1e as a consequence of its small size with respect to the sliding window width.

computed assuming an infinite half-space magnetized source limited by the seafloor and bearing a unit magnetization, and the geometry of the experiment. A comparison is performed within a series of sliding windows and quantified by the coherency between the two signals [Honsho et al., 2009]. A high coherency means similar modeled and observed anomalies on the considered window. For a high enough coherency, the ratio between the observed and synthetic signals (for selected wavelengths in the spectral domain: admittance) corresponds to the absolute magnetization of the near seafloor, i.e., the part of the seafloor which topography and uneven vehicle tracks produce the observed anomaly. The phase shift between the observed and synthetic signals is generally close to 0 or 180° and represents the (normal or reversed) polarity of this magnetization. Other values are sometimes observed, for either geological reasons—e.g., tilted blocks—or computational ones—e.g., partial fit of the observed and synthetic anomalies. The polarity provides useful indications on the age of volcanic structures, as a reverse polarity will certainly characterize features older than the last polarity reversal (0.78 Ma [Cande and Kent, 1995]).

This method has been designed to analyze DSS dives cutting across elongated structures [Honsho et al., 2009], and the synthetic anomalies are computed assuming 2-D infinite sources perpendicular to the dive path. It does not take the surrounding bathymetry into account, an assumption suitable for linear dives crossing relatively flat environments or 2-D structures, but a severe limitation for sinuous dives over 3-D magnetic sources. In such instances, the influence of the various geological structures bounding the dive path cannot be neglected.

We improved the Honsho et al. [2009] method by taking the local bathymetry into consideration, in order to get a more adequate synthetic signal. The high-resolution, 0.5 × 0.5 m bathymetric grid provided by the AUV is resampled as to provide a set of prisms with a 2 × 2 m square section, an infinite depth, and a unit magnetization for forward modeling. For each magnetic measurement point of the DSS, we sum the effect of all prisms located within a given square to get the synthetic magnetic anomaly at that point. For a DSS altitude varying between 0 and 10 m above the seafloor, a 100 × 100 m square centered on the DSS (filled by 2500 2 × 2 m prisms) insures a proper convergence of the calculation. As the intensity of magnetic anomalies decreases with the cube of the distance, the effect of prisms located at the edge of the square is less than 0.7% of that of a prism located beneath the submersible. The width of the computation area should be increased for a higher-altitude survey. Aside from this improvement, the method is similar to the 2-D approach of Honsho et al. [2009].

In both 2-D and 3-D approaches, the magnetization is estimated only for sliding windows with a coherency higher than 0.3. Selecting the proper width of the sliding window is also a matter of investigation. For this

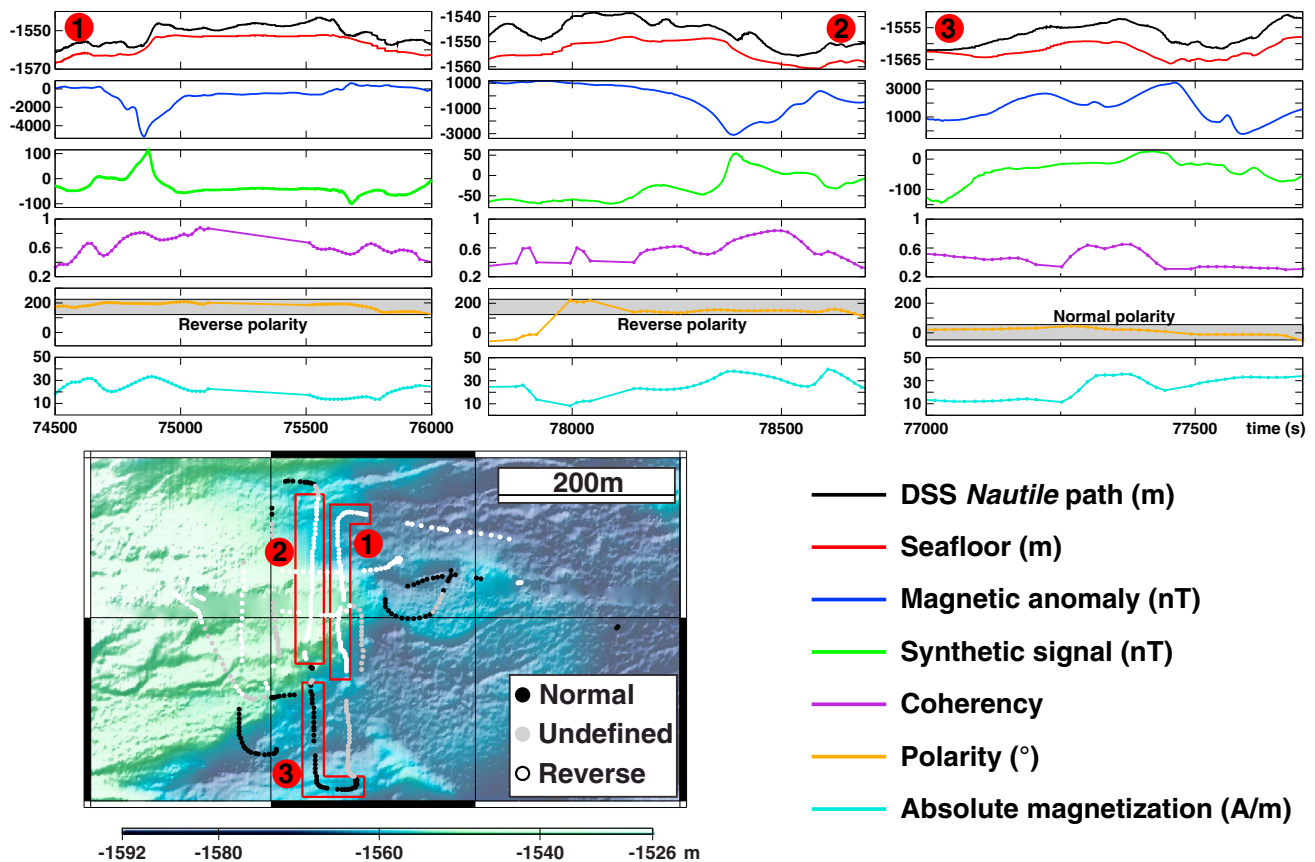


Figure 2. (top) Detailed analysis of three areas characterized by reversed (1 and 2) or normal (3) polarities, with (from top to bottom) geometry of the experiment, observed magnetic anomaly, modeled magnetic anomaly, coherency, polarity, and absolute magnetization. See text for details. (bottom) High-resolution bathymetry with location of the three areas (red contours) and the magnetic polarities obtained for 70 m wide sliding windows and coherency higher than 0.3. Black, white, and grey dots correspond to normal, reversed, and undefined polarities, respectively. Consistency of the polarities at crossings confirms their reliability.

study, we consider 70 and 140 m wide sliding windows (respectively, 512 and 1024 measurements at the average speed of the submersible). The interval between consecutive windows is set to 6 m. Such a large overlap of the sliding windows increases the number of magnetization estimates and allows testing the repeatability (and therefore the reliability) of the results. Magnetization and polarity distributions estimated with different widths of the sliding window are presented in Figures 1b and 1d and Figures 1c and 1e (respectively, for 70 m and 140 m wide sliding windows). The difference between absolute magnetizations computed for these two window lengths is also shown (Figure 1f) to underline the shorter wavelengths obtained while considering 70 m wide sliding windows. We adopt this value and test the reliability of the method on several areas characterized by either normal or reverse polarities, and discuss the origin of such polarities.

4. Results

This method is applied to data collected on a dive of DSS Nautila over a small, ~100 m wide hydrothermal site where active chimneys as high as 6–7 m, diffusion zones, and inactive chimneys were observed, and a maximum fluid temperature of 265°C was measured. On this dive, the submersible followed six roughly parallel N-S profiles spaced ~40 m apart, complemented by three crossing lines, in a design well suited for potential field measurements. Three of the N-S profiles cross the main active hydrothermal area, where they display a lack of magnetization (Figure 1d). This result is consistent with previous findings on basalt-hosted hydrothermal sites [Tivey *et al.*, 1993; Tivey and Johnson, 2002; Tivey and Dymont, 2010; Zhu *et al.*, 2010; Nakamura *et al.*, 2013; Caratori-Tontini *et al.*, 2012; Honsho *et al.*, 2013; Szitkar *et al.*, 2014a]. In addition, tiny areas of low magnetization are observed both in the western and southern parts of the survey,

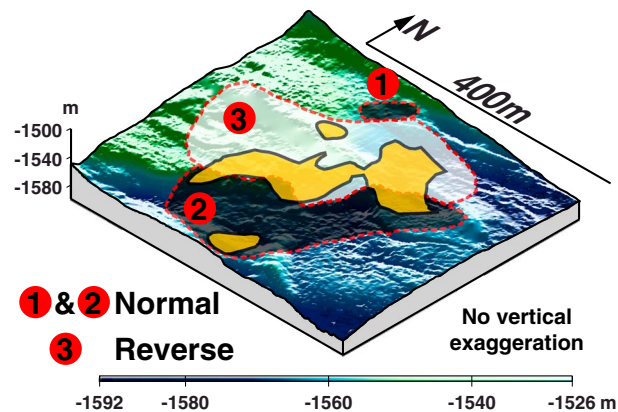


Figure 3. Hydrothermal area as deduced from the low-magnetization intensity (yellow), normal, and reversed polarity areas (respectively black and white) draped on the high-resolution bathymetry. The hydrothermal area and lava flows with different magnetic polarities are uncorrelated.

where small active hydrothermal sites have also been discovered. Their small dimensions (40×30 m) with respect to the size of the sliding window explain their weaker signature in terms of absolute magnetization, compared to the main hydrothermal area. The surrounding area presents strong absolute magnetization values ranging between 10 and 20 A/m, in agreement with the magnetization of fresh basalt [e.g., Wooldridge *et al.*, 1990]. The westernmost and easternmost parts of the survey are associated with a stronger magnetization (>30 A/m), probably corresponding to the most recent lava flows (Figure 1d).

Previous magnetic studies on basalt-hosted hydrothermal sites explain the lack of magnetization as a consequence of thermal

demagnetization (i.e., a temperature higher than 150–200°C, the Curie temperature of titanomagnetite [e.g., Tivey *et al.*, 1993]), hydrothermal alteration of the magnetic minerals (i.e., the transformation of titanomagnetite to the less magnetic titanomaghemite [e.g., Tivey and Johnson, 2002]), or the presence of nonmagnetic sulfide keeping the magnetized layer away from the magnetometer [Szitkar *et al.*, 2014a; Sitkar and Dymont, 2015]. The equivalent magnetizations obtained by various inversion methods are unable to determine whether basalt-hosted hydrothermal sites are marked by low or null values of the magnetization, i.e., if the magnetization is simply attenuated or totally absent. The absolute magnetization obtained by our new method reveals that the shallow seafloor is fully nonmagnetic on a few meters to tens of meters, depending on the altitude of the measurement. This nonmagnetic layer would correspond to the sulfide deposits and/or the stockwork zone of basalt-hosted hydrothermal sites [e.g., Zhao *et al.*, 1998]. Any thermally demagnetized zone or hydrothermal alteration pipe located at greater depths do not have any significant effect on the measurement and cannot be discarded with the available data. Our study points out the presence of nonmagnetic sulfide deposits and/or stockwork zone as a significant cause of the low magnetization recognized at the basalt-hosted hydrothermal sites, especially for measurements made at low altitude.

Both normal and reversed magnetic polarities are observed in the survey area, suggesting a complex history of accumulating volcanic flows. The southern and eastern parts of the survey display a normal polarity; the central, western, and northern parts are dominantly reversed, except for the northern tip where some normal polarities are obtained (Figure 1b). These polarity zones are generally defined from several profiles, both N-S and E-W (Figure 2), and appear to be robust for varying sizes of the sliding windows (Figures 1b and 1c). They do not coincide with the hydrothermal area, which overlap the edge of the main normal and reversed polarity areas (Figure 3).

5. Discussion

Unlike other inversion methods, our approach allows estimating the absolute magnetization of the shallow seafloor and alleviates the determination of an annihilator. For each sliding window, given the topography and the submersible track, we determine the best value of the magnetization contrast between the rock and the water, i.e., the magnetization of the rock, assumed to be constant at the scale of the window for the sake of calculation. We subsequently ascribe this magnetization value to the center of the window. The method requires significant topography and/or variation of the submersible altitude in order to produce meaningful results. Beyond the specific case of a flat topography and a constant altitude survey, a submersible path can be determined for which, given the seafloor topography and a constant magnetization, no magnetic anomaly is observed. Such a “neutral path” is quite similar to the annihilator of other inversion methods, i.e., a distribution of equivalent magnetization that—given the geometry of the acquisition—generates no

magnetic anomaly. In order to produce a strong-enough modeled anomaly, the submersible tracks should significantly divert from the neutral path. Some of the observed low coherency values may be due to such a lack of signal in the modeled anomalies. In each window, the method computes the magnetization as the ratio of observed versus modeled anomalies: a lack of signal on the modeled anomaly results in an undetermined magnetization, but a lack of signal on the observed anomalies means a null magnetization (if the modeled anomaly exhibits a strong-enough signal).

A similar discussion concerns the polarity determinations and their reliability. If both observed and modeled signals are strong, their comparison is easy and their phase shift provides a reliable estimate of the polarity, as shown by the normal and reversed examples in Figure 2. Conversely, if the observed anomaly is weak, the comparison may not be significant, leading to uncertain phase shift and unstable polarity estimates. It may be the case in the demagnetized areas observed at the basalt-hosted hydrothermal sites, which displays less stable polarities (Figure 2).

The size of the sliding windows plays an important role, as it must be adjusted to obtain a reliable estimation of the coherency between observed and synthetic signals. If the windows are too narrow, the estimate will rely only on a few points and its physical meaning will be questionable. Conversely, good coherency values will be difficult to achieve for too-wide sliding windows. A convenient way to evaluate the uncertainty on magnetization is to compare estimates with different window widths: the difference between magnetizations estimated for 70 and 140 m wide windows shown in Figure 1f suggests that values at the western and eastern ends of the survey are poorly constrained.

The proposed 3-D method is quite demanding, as it requires two independent data sets, here the high-resolution bathymetric grid provided by the multibeam echosounder of the AUV and the magnetic and navigation data of the DSS. A possible difficulty lies in errors in either the AUV bathymetry or in the DSS navigation, resulting in errors in the magnetic anomaly model. Moreover, DSS dives are often very sinuous and therefore poorly suited for magnetization estimation. In addition, the reliability of such estimates can generally not be evaluated, as these dives are usually isolated.

Compared to other inversion methods, the proposed approach shows that in the study area, the shallow subseafloor has no magnetization at the basalt-hosted hydrothermal site, because the sulfide deposits associated with such sites are generally nonmagnetic. Surveys achieved by DSS a few meters above the seafloor do not provide any information on the deeper magnetic structure of the site, for instance an altered zone of lower magnetization [Tivey *et al.*, 1993; Tivey and Johnson, 2002; Szitkar and Dymont, 2015]. To access such deeper structures, magnetic surveys should be carried out at different altitudes above the site.

The various polarities determined in the survey area came as a surprise because it was expected from the fresh volcanic morphology and the lack of sediment cover that the survey area is young, possibly younger than the Brunhes-Matuyama boundary (0.78 Ma). The consistent patch of reversed polarity, 150 m wide and at least 400 m long, is confirmed from several nearby or crossing profiles and likely represents a lava flow erupted under reversed magnetic polarity. Whether it is a short reversed polarity episode within the Brunhes period, the younger part of the Matuyama period following the Jaramillo episode (which the observed normal polarities may be part of), or an older period remains to be determined. The investigated area lies within a wide volcanic province with multiple volcanic centers and no clearly defined spreading center, similar to the Southeast Futuna Volcanic Zone described by Pelletier *et al.* [2001], and it is impossible to estimate its age on structural bases.

6. Conclusion

We collected high-resolution, near-seafloor magnetic data above a small, basalt-hosted hydrothermal site using a deep-sea submersible. As for the results obtained on other similar sites from higher-altitude experiments using a ROV or an AUV [Tivey and Johnson, 2002; Szitkar *et al.*, 2014a], this site exhibits a negative magnetic anomaly a few meters above seafloor. We designed a new approach to estimate the absolute magnetization and magnetic polarity of the shallow subseafloor by comparing the observed anomalies to modeled ones assuming the geometry of the experiment and a unit magnetization intensity. This approach reveals that the shallow part of the hydrothermal site (i.e., the sulfide deposit and/or stockwork zone) has no magnetization. Both normal and reversed polarities are observed in the lava flows surrounding the site, suggesting either that

the latter formed during a short episode of reversed polarity during the Brunhes period or that all the lavas formed earlier, presumably during the Matuyama period. This new approach henceforth provides a way to take full advantage of the high-resolution, near-seafloor magnetic measurements acquired by DSS and improves our knowledge on the magnetic effect of small-scale features.

Acknowledgments

We thank the captain and crew of R/V *L'Atalante*, the technical team of DSS Nautile, and the IFREMER scientific team for excellent work at sea. E. Pelleter successfully led the dive presented in this study. IPGP, CNRS-INSU, IFREMER, and GENAVIR are gratefully acknowledged for their financial and technical support. F.S. was supported by a fellowship funded by IFREMER and CNRS. F.S. collaborated with C.H. during a visit funded by an InterRidge Fellowship. The data presented in this paper have been collected as part of an industrial project and are proprietary. They cannot be released and their precise location cannot be disclosed. The reviewers are gratefully acknowledged. This is IPGP contribution 3609.

The Editor thanks Udo Barckhausen and Maurice Tivey for their assistance in evaluating this paper.

References

- Cande, S. C., and D. V. Kent (1995), Revised calibration of the geomagnetic polarity timescale for the late Cretaceous and Cenozoic, *J. Geophys. Res.*, *100*, 6093–6095, doi:10.1029/94JB03098.
- Caratori-Tontini, F., B. Davy, C. De Ronde, R. W. Embley, M. Leybourne, and M. A. Tivey (2012), Crustal magnetization of Brothers Volcano, New Zealand, measured by autonomous underwater vehicles: Geophysical expression of a submarine hydrothermal system, *Econ. Geol.*, *107*, 1571–1581.
- Guspi, F. (1987), Frequency-domain reduction of potential field measurements to a horizontal plane, *Geoexploration*, *24*, 87–98, doi:10.1016/0016-7142(87)90083-4.
- Honsho, C., J. Dymant, K. Tamaki, M. Ravilly, H. Horen, and P. Gente (2009), Magnetic structure of a slow spreading ridge segment: Insights from near-bottom magnetic measurements on board a submersible, *J. Geophys. Res.*, *114*, B05101, doi:10.1029/2008JB005915.
- Honsho, C., T. Ura, and K. Tamaki (2012), The inversion of deep-sea magnetic anomalies using Akaike's Bayesian information criterion, *J. Geophys. Res.*, *117*, B01105, doi:10.1029/2011JB008611.
- Honsho, C., T. Ura, and K. Kim (2013), Deep-sea magnetic vector anomalies over the Hakurei hydrothermal field and the Bayonnaise knoll caldera, Izu-Ogasawara arc, Japan, *J. Geophys. Res. Solid Earth*, *118*, 5147–5164, doi:10.1002/jgrb.50382.
- Hussenöeder, S. A., M. A. Tivey, and H. Schouten (1995), Direct inversion of potential fields from an uneven track with application to the mid-Atlantic Ridge, *Geophys. Res. Lett.*, *22*, 3131–3134, doi:10.1029/95GL03326.
- International Association of Geomagnetism and Aeronomy Working Group V-MOD (2010), International Geomagnetic Reference Field: The eleventh generation, *Geophys. J. Int.*, *183*, 1216–1230, doi:10.1111/j.1365-246X.2010.04804.x.
- Isezaki, N. (1986), A new shipboard three-component magnetometer, *Geophysics*, *51*, 1992–1998.
- Nakamura, K., T. Toki, N. Mochizuki, M. Asada, J. Ishibashi, Y. Nogi, S. Yoshikawa, J. Miyazaki, and K. Okino (2013), Discovery of a new hydrothermal vent based on an underwater, high-resolution geophysical survey, *Deep Sea Res., Part 1*, *74*, 1–10.
- Parker, R. L., and S. P. Huestis (1974), The inversion of magnetic anomalies in the presence of topography, *J. Geophys. Res.*, *79*, 1587–1594, doi:10.1029/JB079i011p01587.
- Pelletier, B., Y. Lagabrielle, M. Benoit, G. Cabioch, S. Calmant, E. Garel, and C. Guivel (2001), Newly identified segments of the Pacific-Australia plate boundary along the North Fiji transform zone, *Earth Planet. Sci. Lett.*, *193*, 347–358.
- Pilkington, M., and W. E. S. Urquhart (1990), Reduction of potential field data to a horizontal plane, *Geophysics*, *55*, 549–555.
- Szitkar, F., and J. Dymant (2015), Near-seafloor magnetics reveal tectonic rotation and deep structure at TAG (Trans-Atlantic Geotraverse) hydrothermal site (Mid-Atlantic Ridge, 26°N), *Geology*, *43*, 87–90, doi:10.1130/G36086.1.
- Szitkar, F., J. Dymant, Y. Choi, and Y. Fouquet (2014a), What causes low magnetization at basalt-hosted hydrothermal sites? Insights from inactive site Krasnov (MAR 16°38'N), *Geochem. Geophys. Geosyst.*, *15*, 1441–1451, doi:10.1002/2014GC005284.
- Szitkar, F., J. Dymant, Y. Fouquet, C. Honsho, and H. Horen (2014b), The magnetic signature of ultramafic-hosted hydrothermal sites, *Geology*, *42*, 715–718, doi:10.1130/G35729.1.
- Tivey, M. A., and H. P. Johnson (2002), Crustal magnetization reveals subsurface structure of Juan de Fuca Ridge hydrothermal vent fields, *Geology*, *30*, 979–982, doi:10.1130/0091-7613(2002)030<0979:CMRSSO>2.0.CO;2.
- Tivey, M. A., and J. Dymant (2010), The magnetic signature of hydrothermal systems in slow-spreading environments, *AGU Geophys. Monogr. Ser.*, *188*, 43–66.
- Tivey, M. A., P. A. Rona, and H. Schouten (1993), Reduced crustal magnetization beneath the active sulfide mound, TAG hydrothermal field, Mid-Atlantic Ridge, at 26°N, *Earth Planet. Sci. Lett.*, *115*, 101–115, doi:10.1016/0012-821X(93)90216-V.
- Wooldridge, A. L., S. E. Haggerty, P. A. Rona, and C. G. A. Harrison (1990), Magnetic properties and opaque mineralogy of rocks from selected seafloor hydrothermal sites at oceanic ridges, *J. Geophys. Res.*, *95*, 12,351–12,374, doi:10.1029/JB095iB08p12351.
- Zhao, X., B. Housen, P. Solheid, and W. Xu (1998), Magnetic properties of leg 158 cores: The origin of remanence and its relation to alteration and mineralization of the active TAG mound, in *Proceedings of the Ocean Drilling Program, Sci. Results*, vol. 158, edited by P. M. Herzog, pp. 337–351, College Station, Tex.
- Zhu, J., J. Lin, Y. J. Chen, C. Tao, C. R. German, D. R. Yoerger, and M. A. Tivey (2010), A reduced crustal magnetization zone near the first observed active hydrothermal vent field on the Southwest Indian Ridge, *Geophys. Res. Lett.*, *37*, L18303, doi:10.1029/2010GL043542.